15th IFK
Proc. of the 15th International Fluid Power Conference- Symposium

134501

Direct model reference adaptive control (MRAC) augmented frameworks for load pressure and position control of servo-valve controlled hydraulic cylinders

Marcel Steidle

Haeusler AG Duggingen, msteidle@haeusler.com

Patrick Stadler

Haeusler AG Duggingen, pstadler@haeusler.com

Jürgen Weber

Chair of Fluid Mechatronic Systems (Fluidtronic), TU Dresden, juergen.weber@tu-dresden.de

Abstract

Servo-valve controlled hydraulic cylinders are widely used in various industrial applications. These systems show highly nonlinear dynamic behavior which poses significant challenges for control system design. This paper develops two novel adaptive control frameworks for cylinder position and load pressure control to enhance the robustness and stability of these systems. The frameworks are specifically designed to address common issues such as parametric uncertainties, unexpected external disturbances and component wear. Key contributions are the development of a single, adaptive control design for the entire operation range as well as the introduction of an algorithm for seamless transition between adaptive position and load pressure control which improves the frameworks' overall performance and practicality. The proposed control frameworks are validated and tested through both numerical simulations and experiments conducted on a 4-roll plate bending machine. Finally, an experimental comparison between the proposed adaptive controllers and conventional linear and nonlinear controllers is presented. The results demonstrate an improvement in accuracy for both position and load pressure control.

Keywords: industrial hydraulics, 4-roll plate bending machine, adaptive control, Model Reference Adaptive Control (MRAC), valve control, position control, load pressure control

1. Introduction

Hydraulic drives are key components in many industries including robotics, manufacturing, forestry and earthwork. Due to their excellent energy- and power-density, they are often deployed for heavy-duty tasks like metal forming or excavation. These systems commonly operate under harsh and varying environmental conditions over extended periods, leading to significant changes in system behavior throughout a machine's lifetime. This variability presents a considerable challenge for control system design.

To accomplish common control tasks like position and load pressure regulation, linear controllers are predominantly used. Their widespread adaptation is due to their conceptual simplicity, ease of implementation and sole reliance on readily available pressure and position measurements [1, 2]. While manually tuned PID based controllers remain common, more sophisticated linear control techniques, such as state-space control, are becoming more popular. For instance, [3] presents methods for system modeling and their application to linear control design, while [4] describes a method to improve feedforward control by combining physical modeling with measurement-based system identification during commissioning.
Additionally, extensive research has been conducted to address the challenges posed by the highly nonlinear dynamics of hydraulic systems. Different applications of nonlinear control techniques can be found for example in [5, 6, 7, 8, 9, 10]. However, these control designs suffer from drawbacks like the reliance on high-fidelity system models [5, 6] or require a fixed, repeatable process [10]. The development of high-fidelity system models is often resource- and time-intensive, making them less accessible to small and medium sized enterprises and manufacturers of special-machinery. This disadvantage is further exacerbated by the aforementioned parametric uncertainties, which reduce model accuracy and, consequently, the performance of model based control designs. The type and magnitude of these parameter variations are difficult to estimate during the design phase, thus motivating the application of robust and adaptive control techniques.
Since the 1950s, adaptive control has been an ongoing subject of research due to its capabilities in rejecting unforeseen disturbances such as structural damage, component wear or changes in the machine configuration. Today, a wide range of different approaches exist which can be broadly categorized into model-based and data-driven techniques [11]. Purely data-driven methods show increasingly promising results in hydraulic system control as seen in [12] and [13]. However, they often lack physical interpretability which poses a challenge for industrial applications as commissioning and maintenance tasks become increasingly complex and opaque. Therefore, despite this extensive research, a control architecture which simultaneously addresses the challenges of parametric uncertainty and external disturbances while maintaining physical interpretability remains a research gap. This work thus aims to develop two novel, adaptive control frameworks that address this gap. A particular emphasis is placed on the practical integration and applicability of these methods within existing industrial control frameworks.

2. System model

Mathematical system models simplify the development of controller designs and enable an assessment of open- and closed-loop behavior and performance. Especially state-space models are widely used in control theory as they provide an intuitive and physically meaningful system description. These models combine a set of coupled, first order differential equations to describe system dynamics with algebraic equations to determine the system outputs [14]:

$$\begin{aligned} \underline{\dot{x}} &= \underline{f}(\underline{x}, \underline{u}, \underline{\Theta}, t) \\ \underline{y} &= \underline{g}(\underline{x}, \underline{u}, \underline{\Theta}, t) \end{aligned} \tag{2.1}$$

The determination of required system equations is demonstrated using the hydraulic plant shown in Table 2.1. First, the original system is considered. It includes a pressure relief valve on the piston side and a check valve on the rod side of the cylinder. While the pressure relief valve protects the cylinder from overpressure, the check valve prevents underpressure. Both phenomena are typically caused by external disturbances. However, if the control system performs adequately, both components remain inactive and are therefore irrelevant for the control design. Furthermore, the seat valve can also be neglected because it remains open during the entire control cycle. This leads to the simplified hydraulic scheme shown on the right side of Table 2.1.

Table 2.1: Schematic representation of the hydraulic drive used for bottom roller movement in a 4-roll plate bending machine.
Left: Original system; **Right**: Simplified model for control design

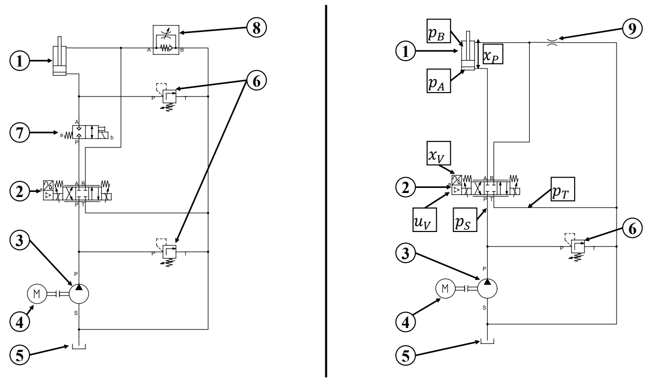

Position	Designation	Position	Designation
1	Differential cylinder	6	Pressure relief valve
2	4/3 proportional valve	7	2/2 seat valve
3	Hydraulic pump	8	Throttle and check valve
4	Electric motor	9	Throttle
5	Hydraulic tank		

To further simplify the model, it is assumed that the supply and tank pressure, p_{S} and p_{T}, are piecewise constant. The resulting model thus requires mathematical descriptions of a 4/3 proportional valve, a differential cylinder and an orifice.
Applying Newtons second law to the cylinder piston one obtains [2]:

$$\ddot{x}_{\mathrm{P}} = \frac{1}{m} \cdot (A_{\mathrm{A}} \cdot p_{\mathrm{A}} - A_{\mathrm{B}} \cdot p_{\mathrm{B}} - F_{\mathrm{f}}(\dot{x}_{\mathrm{P}}) - m \cdot g - F_{\mathrm{ext}}) \tag{2.2}$$

The friction force is given by:

$$F_{\mathrm{f}}(\dot{x}_{\mathrm{P}}) = \sigma \cdot \dot{x}_{\mathrm{P}} + \mathrm{sign}(\dot{x}_{\mathrm{P}}) \cdot \left[F_{\mathrm{c0}} + F_{\mathrm{s0}} \cdot \exp\left(-\frac{\|\dot{x}_{\mathrm{P}}\|}{c_{\mathrm{s}}}\right)\right] \tag{2.3}$$

The external forces vary between different applications of the hydraulic cylinder. For the controller design of a 4-roll plate bending machine, the external forces can be approximated as a mechanical hard stop:

$$F_{\mathrm{ext}}\,(x_{\mathrm{P}}) = \begin{cases} 0, & x_{\mathrm{P}} \leq a \\ k \cdot (x_{\mathrm{P}} - a), & x_{\mathrm{P}} > a \end{cases} \tag{2.4}$$

Using the continuity equation, the pressure dynamics of the cylinder chambers are obtained:

$$\dot{p}_\mathrm{A} = \frac{E\left(p_\mathrm{A}\right)}{V_\mathrm{A}\left(x_\mathrm{P}\right)} \cdot \left(Q_\mathrm{A}\left(p_\mathrm{A}, x_\mathrm{V}\right) - Q_\mathrm{L,i}\left(p_\mathrm{A}, p_\mathrm{B}\right) - Q_\mathrm{L,e,A}\left(p_\mathrm{A}\right) - A_\mathrm{A} \cdot \dot{x}_\mathrm{P}\right) \tag{2.5}$$

$$\dot{p}_\mathrm{B} = \frac{E\left(p_\mathrm{B}\right)}{V_\mathrm{B}\left(x_\mathrm{P}\right)} \cdot \left(Q_\mathrm{B}\left(p_\mathrm{B}, x_\mathrm{V}\right) + Q_\mathrm{L,i}\left(p_\mathrm{A}, p_\mathrm{B}\right) - Q_\mathrm{L,e,B}\left(p_\mathrm{B}\right) + A_\mathrm{B} \cdot \dot{x}_\mathrm{P}\right) \tag{2.6}$$

The chamber volumes and leakage flow rates are defined as:

$$V_\mathrm{A}\left(x_\mathrm{P}\right) = V_\mathrm{0,A} + A_\mathrm{A} \cdot x_\mathrm{P} \quad \text{and} \quad V_\mathrm{B}\left(x_\mathrm{P}\right) = V_\mathrm{0,B} + A_\mathrm{B} \cdot \left(S - x_\mathrm{P}\right)$$

$$Q_\mathrm{L,i}\left(p_\mathrm{A}, p_\mathrm{B}\right) = k_\mathrm{L,i} \cdot \left(p_\mathrm{A} - p_\mathrm{B}\right) \quad \text{and} \quad Q_\mathrm{L,e,A/B}\left(p_{A/B}\right) = k_\mathrm{L,e,A/B} \cdot \left(p_{A/B} - p_0\right)$$

The flow rates for both cylinder chambers are given by:

$$Q_\mathrm{A}\left(p_\mathrm{A}, x_\mathrm{V}\right) = Q_\mathrm{V,A}\left(p_\mathrm{A}, x_\mathrm{V}\right) \quad \text{and} \quad Q_\mathrm{B}\left(p_\mathrm{B}, x_\mathrm{V}\right) = Q_\mathrm{O}\left(p_\mathrm{B}\right) + Q_\mathrm{V,B}\left(p_\mathrm{B}, x_\mathrm{V}\right)$$

With the flow rates through the orifice and 4/3 proportional valve:

$$Q_\mathrm{O}\left(p_\mathrm{B}\right) = k_\mathrm{O} \cdot \operatorname{sign}\left(p_\mathrm{T} - p_\mathrm{B}\right) \cdot \sqrt{\left\|p_\mathrm{T} - p_\mathrm{B}\right\|} \tag{2.7}$$

$$Q_\mathrm{V,A}\left(p_\mathrm{A}, x_\mathrm{V}\right) = k_\mathrm{V,A} \cdot \begin{cases} \operatorname{sign}\left(p_\mathrm{S} - p_\mathrm{A}\right) \cdot \sqrt{\left\|p_\mathrm{S} - p_\mathrm{A}\right\|} \cdot x_\mathrm{V}, & x_\mathrm{V} \geq 0 \\ \operatorname{sign}\left(p_\mathrm{T} - p_\mathrm{A}\right) \cdot \sqrt{\left\|p_\mathrm{T} - p_\mathrm{A}\right\|} \cdot \left(-x_\mathrm{V}\right), & x_\mathrm{V} < 0 \end{cases} \tag{2.8}$$

$$Q_\mathrm{V,B}\left(p_\mathrm{B}, x_\mathrm{V}\right) = k_\mathrm{V,B} \cdot \begin{cases} \operatorname{sign}\left(p_\mathrm{T} - p_\mathrm{B}\right) \cdot \sqrt{\left\|p_\mathrm{T} - p_\mathrm{B}\right\|} \cdot x_\mathrm{V}, & x_\mathrm{V} \geq 0 \\ \operatorname{sign}\left(p_\mathrm{S} - p_\mathrm{B}\right) \cdot \sqrt{\left\|p_\mathrm{S} - p_\mathrm{B}\right\|} \cdot \left(-x_\mathrm{V}\right), & x_\mathrm{V} < 0 \end{cases} \tag{2.9}$$

To further simplify the model for control design, the following assumptions are made:

- No leakage flows $Q_\mathrm{L,i} = Q_\mathrm{L,e,A/B} = 0$
- The bulk modulus is constant $E\left(p_\mathrm{A}\right) = E\left(p_\mathrm{B}\right) = \mathrm{cst.}$
- The dynamic behavior of the valve spool is neglected $x_\mathrm{V} = u_\mathrm{V}$
- The valve has no overlap
- Only viscous friction is considered $F_\mathrm{f}\left(\dot{x}_\mathrm{P}\right) = \sigma \cdot \dot{x}_\mathrm{P}$

Defining the state vector $\underline{x} = \begin{bmatrix} x_\mathrm{P} & \dot{x}_\mathrm{P} & p_\mathrm{A} & p_\mathrm{B} \end{bmatrix}^\mathsf{T}$, the disturbance as $d = F_\mathrm{ext}$ and the input as $u = u_\mathrm{V}$ and combining equations 2.2, 2.5 and 2.6 one obtains the state-space representation:

$$\dot{\underline{x}} = \begin{pmatrix} x_2 \\ \frac{1}{m} \cdot \left(A_\mathrm{A} \cdot x_3 - A_\mathrm{B} \cdot x_4 - m \cdot g - \sigma \cdot x_2\right) \\ \frac{E}{V_\mathrm{A}(x_1)} \cdot \left(Q_\mathrm{A}\left(x_3, u\right) - A_\mathrm{A} \cdot x_2\right) \\ \frac{E}{V_\mathrm{B}(x_1)} \cdot \left(Q_\mathrm{B}\left(x_4, u\right) + A_\mathrm{B} \cdot x_2\right) \end{pmatrix} + \begin{pmatrix} 0 \\ -\frac{1}{m} \\ 0 \\ 0 \end{pmatrix} \cdot d \tag{2.10}$$

While measurements of the cylinder position and both chamber pressures are available, the output equation differs based on the current control task:

$$y_\mathrm{Pos} = x_1 \qquad\qquad y_\mathrm{Load} = x_3 - \frac{A_\mathrm{B}}{A_\mathrm{A}} \cdot x_4 \tag{2.11}$$

3. Controller design

This section presents two different methods to design adaptive controllers for cylinder and load pressure control. Both designs are based on a direct MRAC approach.

3.1. Direct model reference adaptive control (MRAC)

Direct MRAC aims at preserving desirable system behavior in the presence of unexpected parametric variations or disturbances. Therefore, it compares the behavior of a reference model against the real plant. Controller parameters are directly adapted based on the observed error between reference model and plant. Figure 3.1 shows the core components of a direct MRAC approach which are the aforementioned reference model, the adaptation law, the adaptive controller and the base controller.

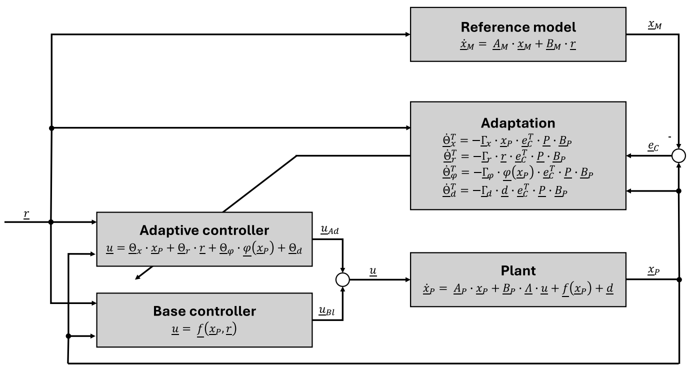

Figure 3.1: Block diagram of direct-MRAC based on the work of [15]

The base controller is designed to stabilize the plant during nominal conditions. If the plant is expected to be linear, the base controller can be designed as [16]:

$$\underline{u} = \underline{M}_{\mathrm{u}} \cdot \underline{r} + \underline{K} \cdot (\underline{M}_{\mathrm{x}} \cdot \underline{r} - \underline{x}) \tag{3.1}$$

Applying this control input to the nominal plant dynamics results in a design method for the reference model:

$$\dot{\underline{x}}_{\mathrm{M}} = \underbrace{\left(\underline{\hat{A}}_{\mathrm{P}} - \underline{\hat{B}}_{\mathrm{P}} \cdot \underline{K}\right)}_{\underline{A}_{\mathrm{M}}} \cdot \underline{x}_{\mathrm{M}} + \underbrace{\underline{\hat{B}}_{\mathrm{P}} \cdot (\underline{M}_{\mathrm{u}} + \underline{K} \cdot \underline{M}_{\mathrm{x}})}_{\underline{B}_{\mathrm{M}}} \cdot \underline{r} \tag{3.2}$$

If the real system deviates from the reference model, the adaptation mechanism becomes active. The choice of the adaptation mechanism and the appropriate control law depends on the nature of the expected disturbances. A general approach can be seen in Figure 3.1. However, if the disturbance is expected to be highly nonlinear, the following control law is sufficient:

$$\underline{u}_{\mathrm{Ad}} = \underline{\Theta}_{\varphi} \cdot \underline{\varphi}\left(\underline{x}_{\mathrm{P}}\right) + \underline{\Theta}_{\mathrm{d}} \tag{3.3}$$

The regressor vector $\underline{\varphi}\left(\underline{x}\right)$ can either be derived from physical system knowledge or by approximation, commonly using a single hidden layer neural network [17].

3.2. Type I: Feedback linearization

For the application of direct MRAC, models with a nearly linear behavior are preferred. Furthermore, control design for this type of models is comparatively straightforward as a broad variety of well-founded control design methods is available. While methods for linear systems distinguish themselves with verifiable, global stability and robustness measures [16], design methods for nonlinear systems are often cumbersome, require simplifications or provide only limited insight into the closed-loop system behavior. This motivates the application of feedback linearization, a technique that transforms a nonlinear system into a linear one, thereby enabling the use of well established linear control methods for nonlinear systems. This is achieved by a state transformation $\underline{z} = \underline{\Phi}\left(\underline{x}\right)$. If the state transformation $\underline{\Phi}\left(\underline{x}\right)$ is a local diffeomorphism around a workpoint $\underline{x}_0$ and the system description is affine in $\underline{u}$, application of the state transformation renders the system linear in the new state description $\underline{z}$ [18].
In order to use feedback linearization, the nonlinear system has to be expressed in the form:[1]

$$\begin{aligned} \dot{\underline{x}} &= \underline{f}\left(\underline{x}\right) + \underline{g}\left(\underline{x}\right) \cdot u \\ y &= h\left(\underline{x}\right) \end{aligned} \tag{3.4}$$

To determine the new state variables $\underline{z}$, the output equation is differentiated in time until the r-th derivative of y shows a direct dependency on u. Defining the states $\underline{\xi} = \begin{bmatrix} y & \dot{y} & \dots & y^{(r-1)} \end{bmatrix}^{\mathsf{T}}$ and the new input $v = y^{(r)}$, a linear model is obtained:

$$\begin{aligned} \dot{\underline{\xi}} &= \underbrace{\begin{pmatrix} 0 & 1 & 0 & \dots & 0 \\ 0 & 0 & \ddots & \ddots & 0 \\ 0 & \dots & 0 & \ddots & 0 \\ 0 & & \dots & 0 & 1 \\ 0 & & \dots\dots & & 0 \end{pmatrix}}_{\underline{\tilde{A}}} \cdot \underline{\xi} + \underbrace{\begin{pmatrix} 0 \\ \vdots \\ \vdots \\ 0 \\ 1 \end{pmatrix}}_{\underline{\tilde{b}}} \cdot v \\ y &= \underbrace{\begin{bmatrix} 1 & 0 & \dots & 0 \end{bmatrix}}_{\underline{\tilde{c}}} \cdot \underline{\xi} \end{aligned} \tag{3.5}$$

Controller design for the system given by Equation 3.5 can be done for example by using pole-placement or linear quadratic regulation (LQR). To obtain the input to the nonlinear system, following transformation based on the Lie-derivatives has to be applied [18]:

$$u = \frac{v - L_{\underline{f}}^{r} h\left(\underline{x}\right)}{L_{\underline{g}} L_{\underline{f}}^{r-1} h\left(\underline{x}\right)} \tag{3.6}$$

However, Equation 3.5 only represents the entire, original system if the relative degree r equals the number of states. Otherwise, the system possesses $(n_x - r)$ states $\underline{\eta}$ which are not influenced by the control input and thus can not be stabilized by the control system. Therefore, these states have to be inherently stable to guarantee stability of the entire system. Determination of the zero dynamics can be achieved through two distinct approaches [18]:

[1]The following discussion focuses on SISO-systems. For discussions of the MIMO case refer e.g. to [18] or [19]

1. Solving the partial differential equations $\frac{\partial \eta_i}{\partial t} = \frac{\partial \Phi_{r+i}(\underline{x})}{\partial \underline{x}} \cdot \left(\underline{f}\left(\underline{x}\right) + \underline{g}\left(\underline{x}\right) \cdot u\right)$
2. Selecting them arbitrarily and checking if $\det\left(\frac{\partial \Phi(\underline{x})}{\partial \underline{x}}\right) \neq 0$

Table 3.1: Results of feedback linearization for position and load pressure control applied to the state space system described by equations 2.10 and 2.11

	Position	**Load pressure**
Controllable states	$\xi_1 = x_1$ $\xi_2 = x_2$ $\xi_3 = \frac{1}{m} \cdot (A_{\mathrm{A}} \cdot x_3 - A_{\mathrm{B}} \cdot x_4 - m \cdot g - \sigma \cdot x_2)$	$\xi_1 = x_3 - \frac{A_{\mathrm{B}}}{A_{\mathrm{A}}} \cdot x_4$
Zero dynamics	$\eta_1 = x_3 - \frac{A_{\mathrm{B}}}{A_{\mathrm{A}}} \cdot x_4$ $\eta_2 = x_3$	$\eta_1 = x_1$ $\eta_2 = x_2$ $\eta_3 = \frac{1}{m} \cdot (A_{\mathrm{A}} \cdot x_3 - A_{\mathrm{B}} \cdot x_4 - m \cdot g - \sigma \cdot x_2)$ $\eta_4 = x_3$
Linear system	$\dot{\underline{\xi}} = \begin{pmatrix} 0 & 1 & 0 \\ 0 & 0 & 1 \\ 0 & 0 & 0 \end{pmatrix} \cdot \underline{\xi} + \begin{pmatrix} 0 \\ 0 \\ 1 \end{pmatrix} \cdot v$	$\dot{\xi} = v$
Lie-derivatives	$L_{\underline{f}}^{r} h\left(\underline{x}\right) = \frac{1}{m} \cdot$ $\Big[- \frac{E}{V_A\left(x_1\right)} \cdot A_A^2 \cdot x_2$ $- \frac{E}{V_B\left(x_1\right)} \cdot A_B \cdot \left(Q_O\left(x_4\right) + A_B \cdot x_2\right)$ $- \frac{\sigma}{m} \cdot \left(A_A \cdot x_3 - A_B \cdot x_4 - mg - \sigma \cdot x_2\right)\Big]$ $L_{\underline{g}} L_{\underline{f}}^{r-1} h\left(\underline{x}\right) = \frac{1}{m} \cdot$ $\Big[\frac{E}{V_{\mathrm{A}}\left(x_1\right)} \cdot A_{\mathrm{A}} \cdot Q_{\mathrm{V,A,nom}}\left(x_3\right)$ $- \frac{E}{V_{\mathrm{B}}\left(x_1\right)} \cdot A_{\mathrm{B}} \cdot Q_{\mathrm{V,B,nom}}\left(x_4\right)\Big]$	$L_{\underline{f}}^{r} h\left(\underline{x}\right) =$ $- \frac{E}{V_A\left(x_1\right)} \cdot A_A \cdot x_2$ $- \frac{A_B}{A_A} \cdot \frac{E}{V_B\left(x_1\right)} \cdot \left[Q_O\left(x_4\right) + A_B \cdot x_2\right]$ $L_{\underline{g}} L_{\underline{f}}^{r-1} h\left(\underline{x}\right) =$ $\frac{E}{V_{\mathrm{A}}\left(x_1\right)} \cdot Q_{\mathrm{V,A,nom}}\left(x_3\right)$ $- \frac{A_{\mathrm{B}}}{A_{\mathrm{A}}} \cdot \frac{E}{V_{\mathrm{B}}\left(x_1\right)} \cdot Q_{\mathrm{V,B,nom}}\left(x_4\right)$
Interpretation	• States represent position, velocity and acceleration • Control input represents jerk • Cylinder pressures are not controllable. They result from the current velocity and external load.	• System is scalar and represents load pressure dynamics. • Other states are only considered during input transformation

Unfortunately, the system description in Equation 2.10 is not affine in the control variable as the flow rate through the proportional valve is more involved. However, equations 2.8 and 2.9 can be rewritten as:

$$Q_{\mathrm{V,A}}\left(x_3, u\right) = Q_{\mathrm{V,A,nom}}\left(x_3, u\right) \cdot u \quad \text{and} \quad Q_{\mathrm{V,B}}\left(x_4, u\right) = Q_{\mathrm{V,B,nom}}\left(x_4, u\right) \cdot u \tag{3.7}$$

With:

$$Q_{\mathrm{V,A,nom}}(x_3,u) = k_{\mathrm{V,A}} \cdot \begin{cases} \mathrm{sign}\left(p_{\mathrm{S}} - x_3\right) \cdot \sqrt{\|p_{\mathrm{S}} - x_3\|}, & u \geq 0 \\ -\mathrm{sign}\left(p_{\mathrm{T}} - x_3\right) \cdot \sqrt{\|p_{\mathrm{T}} - x_3\|}, & u < 0 \end{cases}$$
$$Q_{\mathrm{V,B,nom}}(x_4,u) = k_{\mathrm{V,B}} \cdot \begin{cases} \mathrm{sign}\left(p_{\mathrm{T}} - x_4\right) \cdot \sqrt{\|p_{\mathrm{T}} - x_4\|}, & u \geq 0 \\ -\mathrm{sign}\left(p_{\mathrm{S}} - x_4\right) \cdot \sqrt{\|p_{\mathrm{S}} - x_4\|}, & u < 0 \end{cases} \tag{3.8}$$

Using Equation 3.7, the system becomes affine in the control variable if $u > 0$ or if $u < 0$. Thereby, if the system description is separated around $u = 0$, it satisfies Equation 3.4 which justifies the usage of feedback linearization.
An overview of the feedback linearized systems can be found in Table 3.1. It can be seen that the zero dynamics of the position and load pressure controller are selected in a way that both scenarios use the same transformed state representation.
Combining feedback linearization with model reference adaptive control leads to the control scheme shown in Figure 3.2a. In this context, the adaptive controller acts on the transferred states. Thereby, it needs to compensate for uncertainties and deviations in the state and input transformation. These errors are usually nonlinear. Therefore, the control law given by Equation 3.3 is used for MRAC. As the proposed position and load pressure controller share the same state representation and act on the same system, both control systems are affected by the same disturbances and uncertainties. For this reason, a transfer of adapted controller gains between both controllers is desirable.
To transfer the gains between both controllers, it is further assumed that they share the same regressor vector $\underline{\varphi}(\underline{x})$. Based on the idea of bumpless transfer, it is assumed that at the time of controller switching t_s both controllers should produce the same output:

$$u_{\mathrm{Pos}}(t_{\mathrm{s}}) \overset{!}{=} u_{\mathrm{Load}}(t_{\mathrm{s}}) \tag{3.9}$$

Separating the output of the base and adaptive controller in Equation 3.6 one obtains:

$$u_i(t_{\mathrm{s}}) = \underbrace{\frac{v_{\mathrm{Bl},i} - L_{\underline{f}}^{r_i} h_i(\underline{x})}{L_{\underline{g}} L_{\underline{f}}^{r_i - 1} h_i(\underline{x})}}_{\text{Base controller}} + \underbrace{\frac{v_{\mathrm{Ad},i}}{L_{\underline{g}} L_{\underline{f}}^{r_i - 1} h_i(\underline{x})}}_{\text{Adaptive controller}} \tag{3.10}$$

Combining equations 3.3, 3.9 and 3.10 and solving for the adaptive control input of the load pressure controller results in:

$$\begin{gathered} \underline{\Theta}_{\varphi,\mathrm{Load}} \cdot \underline{\varphi}(\underline{x}) + \Theta_{\mathrm{d,Load}} = \\ \frac{L_{\underline{g}} L_{\underline{f}}^{r_{\mathrm{Load}}-1} h_{\mathrm{Load}}(\underline{x})}{L_{\underline{g}} L_{\underline{f}}^{r_{\mathrm{Pos}}-1} h_{\mathrm{Pos}}(\underline{x})} \cdot \underline{\Theta}_{\varphi,\mathrm{Pos}} \cdot \underline{\varphi}(\underline{x}) + \Delta u_{\mathrm{Bl}} + \frac{L_{\underline{g}} L_{\underline{f}}^{r_{\mathrm{Load}}-1} h_{\mathrm{Load}}(\underline{x})}{L_{\underline{g}} L_{\underline{f}}^{r_{\mathrm{Pos}}-1} h_{\mathrm{Pos}}(\underline{x})} \cdot \Theta_{\mathrm{d,Pos}} \end{gathered} \tag{3.11}$$

With:

$$\Delta u_{\mathrm{Bl}} = L_{\underline{g}} L_{\underline{f}}^{r_{\mathrm{Load}}-1} h_{\mathrm{Load}}(\underline{x}) \cdot \left[\frac{v_{\mathrm{Bl,Pos}} - L_{\underline{f}}^{r_{\mathrm{Pos}}} h_{\mathrm{Pos}}(\underline{x})}{L_{\underline{g}} L_{\underline{f}}^{r_{\mathrm{Pos}}-1} h_{\mathrm{Pos}}(\underline{x})} - \frac{v_{\mathrm{Bl,Load}} - L_{\underline{f}}^{r_{\mathrm{Load}}} h_{\mathrm{Load}}(\underline{x})}{L_{\underline{g}} L_{\underline{f}}^{r_{\mathrm{Load}}-1} h_{\mathrm{Load}}(\underline{x})} \right]$$

Using coefficient comparison results in:

$$\underline{\Theta}_{\varphi,\mathrm{Load}} = \frac{L_{\underline{g}} L_{\underline{f}}^{r_{\mathrm{Load}}-1} h_{\mathrm{Load}}\left(\underline{x}\right)}{L_{\underline{g}} L_{\underline{f}}^{r_{\mathrm{Pos}}-1} h_{\mathrm{Pos}}\left(\underline{x}\right)} \cdot \underline{\Theta}_{\varphi,\mathrm{Pos}} \tag{3.12}$$

$$\Theta_{\mathrm{d,Load}} = \Delta u_{\mathrm{Bl}} + \frac{L_{\underline{g}} L_{\underline{f}}^{r_{\mathrm{Load}}-1} h_{\mathrm{Load}}\left(\underline{x}\right)}{L_{\underline{g}} L_{\underline{f}}^{r_{\mathrm{Pos}}-1} h_{\mathrm{Pos}}\left(\underline{x}\right)} \cdot \Theta_{\mathrm{d,Pos}} \tag{3.13}$$

Equations 3.12 and 3.13 represent the exchange of obtained knowledge based on adaptation. As these mappings are bijective, transfer in both directions is possible by inverting.

3.3. Type II: Linear replacement model

The main purposes of Type II adaptive control are the preservation of controller performance for industrial applications while simultaneously relying on minimum model knowledge. Therefore, it incorporates arbitrary, existing control frameworks by identification of the closed loop system after commissioning and uses the identified system as reference model. The block diagram of the resulting control scheme can be seen in Figure 3.2b. Compared to the scheme of Type I, Type II is distinguished by a reduced complexity as it avoids the additional state transformation.

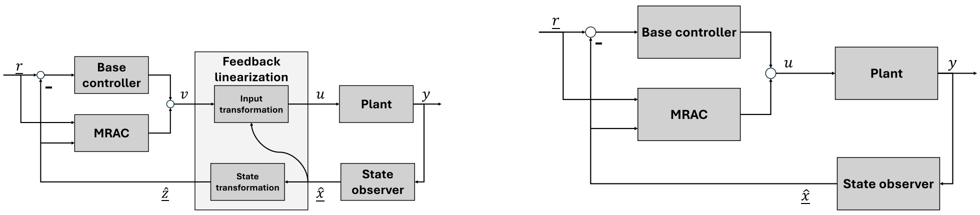

(a) Adaptive control type I

(b) Adaptive control type II

Figure 3.2: Block diagrams of adaptive control frameworks

Additionally, Type II adaptive control integrates smoothly into existing commissioning routines as can be seen by the following, recommended sequence:

1. Commissioning of the known control framework
2. Collecting data from the closed-loop system
   - The collected data should represent system behavior over the entire operating range.
   - Data collection requires movement in closed loop mode.
   - The set and actual values of the controlled output should be recorded.
3. Identification of a black box model using for example least squares or maximum likelihood estimation
4. Defining the identified model as reference model for direct MRAC
5. Parametrization of the adaptation behavior

Examples for the results of system identification can be seen in Figure 3.3. Hereby, the positioning behavior of the actuator is modeled as a PT2 element while the pressure dynamics are approximated as PT1 model. Since the identified model does not incorporate any information about the underlying system physics, all deviations from the nominal performance are compensated by adaptation of the controller. This complicates error tracking as intended system variations like changing supply pressures have to be compensated by the base controller. Otherwise they appear as disturbance to the adaptive controller and lead to adaptation of the control law.

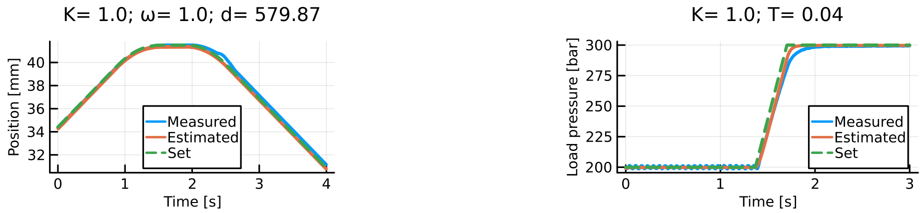

(a) Identified PT2 position model

(b) Identified PT1 load pressure model

Figure 3.3: Results of closed-loop system identification

4. Simulation results

Simulation based design is nowadays standard in research and industry as it provides a cost and time efficient way to validate and test new concepts. Furthermore, it allows for system evaluation under wide parametric variations or under safety critical conditions. For this work, an open-source simulation environment developed in *julia* [20] is used, leveraging the *DifferentialEquations.jl* [21] and *ModellingToolkit.jl* [22] packages for acausal, symbol-based modeling and control design.
For evaluation of the control performance the following test scenarios are evaluated:

1. Load pressure control with suddenly increasing cylinder leakage
2. Position and load pressure control with different supply pressure control schemes
3. Switching between adaptive position and load pressure control

All scenarios use a common system model which is based on the experimental setup presented in Section 5. The nominal parameter values are listed in Table 4.1.

Table 4.1: Nominal parameters of the simulated cylinder

Parameter	**Unit**	**Value**	**Parameter**	**Unit**	**Value**
Piston side area A_A	mm^2	3848.5	Piston rod side area A_B	mm^2	1885.0
Piston stroke S	mm	85.0	Viscous friction coefficient σ	$\frac{\mathrm{N}}{\frac{\mathrm{mm}}{\mathrm{s}}}$	192.0
Piston mass m_P	kg	2.96	Load mass m_L	kg	475.6
Flow rate coefficient valve k_V	$\frac{1}{\mathrm{min}\cdot\sqrt{\mathrm{bar}}}$	0.338	Flow rate coefficient orifice k_O	$\frac{1}{\mathrm{min}\cdot\sqrt{\mathrm{bar}}}$	0.0
Flow rate coefficient internal lekage $k_{L,i}$	$\frac{1}{\mathrm{min}\cdot\mathrm{bar}}$	0.0	Flow rate coefficient external lekage $k_{L,e}$	$\frac{1}{\mathrm{min}\cdot\mathrm{bar}}$	0.0
Supply pressure p_S	bar	310.0	Tank pressure p_T	bar	2.0
Bulk modulus E	bar	18000.0			

The first scenario examines the control performance of Type I adaptive control under unexpected disturbances. Therefore, an additional 2-way valve is introduced between the piston and ring side of the cylinder. Activating the 2-way valve leads to an unexpected flow rate between both piston chambers which has to be compensated by the controller. To evaluate the performance of the adaptive controller, it is compared against a P-controller, a P-to-PI switching control structure, where the integral action is added in proximity of the target value, and a nonlinear controller based on feedback linearization. Figure 4.1 shows the results. All designs show a good tracking behavior during the first 9 s. At this point, the disturbance is introduced by opening the 2-way valve. This leads to an immediate decline of control performance for all four designs. The nonlinear controller, in particular, shows the strongest reaction to the disturbance and fails to recover which leads to a sustained steady-state error for the rest of the simulation run. As the adaptive controller is based on the nonlinear controller, it also shows a strong initial reaction to the disturbance. However, due to the adaptation mechanism, it quickly recovers its performance. During the following setpoint changes, the system with adaptive control shows the smallest control deviations. Especially during the transition phases, nonlinear control designs show a significantly improved performance compared to the linear controllers.

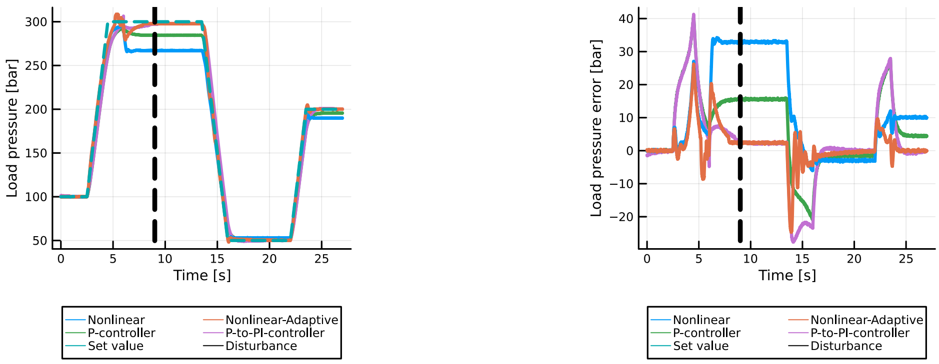

(a) Trajectory

(b) Tracking error

Figure 4.1: Performance of different load pressure controller designs under the influence of an unexpected disturbance caused by a cylinder leakage

In summary, it can be said that nonlinear control designs improve the control performance during nominal conditions. However, their dependence on a sophisticated system model makes them vulnerable against unexpected disturbances or model errors. These disadvantages can be compensated by a nonlinear controller with adaptation, as described in Section 3.2, resulting in the increased performance shown in Figure 4.1.

To further investigate the applicability of adaptive controllers in industrial settings, the second scenario is considered. For this scenario, a total of six different control designs are benchmarked. Similar to the designs of scenario 1, feedback control is achieved using a P-controller, a P-to-PI switching controller and a nonlinear controller based on feedback linearization. Additionally, all three foundational controllers are enhanced by an adaptive layer and the linear position controllers are augmented by a model-based feedforward structure which inverts equations 2.8 and 2.9 to calculate the necessary control input.

During this scenario, the system is disturbed by a varying supply pressure. This represents common practical applications where systems lack a pressure accumulator or utilize load-sensing, which actively modulates the supply pressure. To quantify the influence of changing supply pressures, two control schemes are evaluated:

1. **Constant pressure**: The supply pressure is constantly hold at $310\,\mathrm{bar}$.
2. **Load-Sensing**: Supply pressure is adapted based on the highest moving actuator pressure.

The setpoint trajectories are generated to replicate the operation of the CNC-interface of the test machine in Section 5 and are illustrated in Figure 4.2. Notably, the position setpoint is designed to induce an external force on the cylinder at a position of $40\,\mathrm{mm}$, simulating the contact force between bottom and top rollers of the machine.

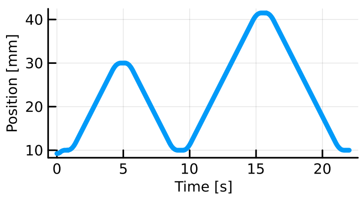

(a) Position

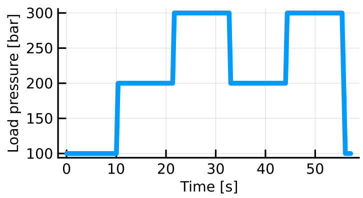

(b) Load pressure

Figure 4.2: Setpoint trajectories used for controller comparison

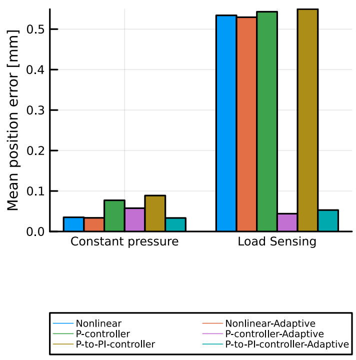

(a) Position

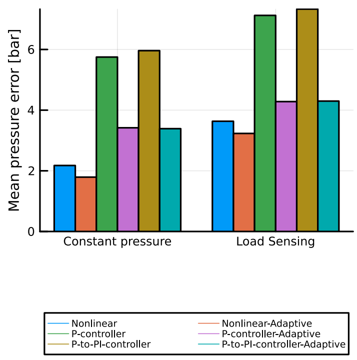

(b) Load pressure

Figure 4.3: Simulated performance of different control designs

Figure 4.3 presents the mean absolute control deviations for both the load pressure and position controllers. It is evident that supply pressure variations significantly degrade control performance. This effect is especially pronounced in the linear controllers without adaptation as they lack an effective mechanism to compensate for supply pressure variations. Consequently, extending these controllers with a Type II adaptive framework leads to a substantial improvement in accuracy by compensating for these variations. The performance of the adaptive position controllers under load-sensing distinctively highlights this effect. Because load-sensing stabilizes the difference between supply and cylinder pressure, the valve flow rate becomes primarily dependent on the control input alone. This reduces system complexity which in turn facilities faster adaptation and improved convergence, leading to enhanced control performance. In contrast, the adaptive enhancement has a reduced influence on the nonlinear controller's performance, as the adaptation process is already significantly affected by the underlying structure of feedback linearization.

In summary, adaptive and nonlinear controllers are both capable of improving accuracy, particularly under varying supply pressures. The Type II adaptive controller design is especially promising, as it significantly enhances the performance of conventional linear controllers.

Finally, the third scenario is examined. As discussed in Section 3.2, transfer of adaptation gains between position and load pressure control is a common and essential task. To validate the increase in controller performance by introduction of the transfer algorithm, the same control task is simulated with and without the switching algorithm. The 2-way valve between both cylinder chambers is open for the entire simulation. During the first 6.2 s, position control is active and adapts for the unexpected flow rate between the cylinder chambers. Thereafter, the controller mode switches from position to pressure control. Results can be seen in Figure 4.4. As expected, the transfer of controller gains significantly reduces the initial control transient after switching, as the previously acquired knowledge about the system's behavior is leveraged by the new controller.

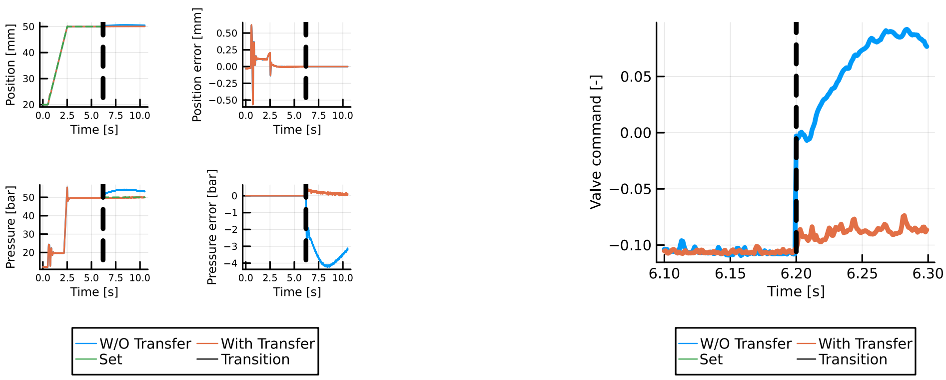

(a) Trajectories and tracking errors

(b) Control input

Figure 4.4: Trajectories and control deviations using adaptation transfer

5. Experimental results

An experimental campaign was designed and executed to validate the novel control approaches by comparing different controller designs. All experiments were conducted on a **4-roll plate bending machine** (HAEUSLER, VRM-2000x23) which can be seen in Figure 5.1. Both side rollers and the bottom roller can be moved linearly using hydraulic actuators while the top and bottom roller are rotary driven by electric motors. Linear movement is conducted via two servo-valve controlled differential cylinders per roller which operate in leader-follower control to synchronize their movements. The required oil for all hydraulic actuators is provided by a **gear pump** (Bosch Rexroth, PGH2-2X/005RE07VU2). As the pump provides a constant flow rate, supply pressure is adjusted between 20 bar to 310 bar via a proportional pressure relief valve. For process and CNC-control, the machine is equipped with a state of the art PLC developed at HAEUSLER AG. The hardware consists of a **4/3-way proportional valve** (Bosch Rexroth, 4WRPEH6C3B02L-3X/M/24A1), an **absolute position encoder** (Baumer, EAL580-B) in combination with a **draw-wire sensor** (MICRO-EPSILON, WDS-2000-P60-M-SO-HAE) and two **pressure transducers** (IFM, PA 9020) per linear axis. Thereby, the machine is capable to perform high precision interpolation-movements between all axes, allowing for the production of complex work pieces with high radius transition requirements.

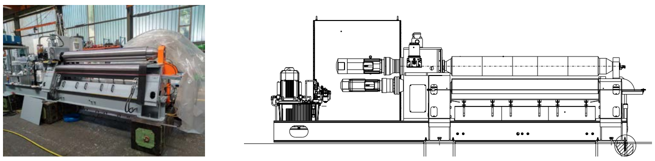

Figure 5.1: Test machine (HAEUSLER, VRM-2000x23) at HAEUSLER AG

For the experimental survey, a total of six different control approaches were benchmarked. These were based on three foundational controllers: the **currently implemented machine controller**, a **newly designed linear switching P-to-PI controller** (derived from scenarios 1 and 2 in Section 4), and a **nonlinear controller based on feedback linearization**. The primary difference between the default machine controller and the new linear controller lies in their feedforward structures. Where the new linear controller employs a model-based feedforward structure described in Section 4, the default machine controller utilizes a one-dimensional characteristic curve that maps the cylinder velocity to the control input. All three foundational controllers were enhanced by an adaptive layer. The two linear controllers were extended using the Type II adaptive framework (see Section 3.3), while the nonlinear controller was augmented with the Type I adaptive framework (see Section 3.2).

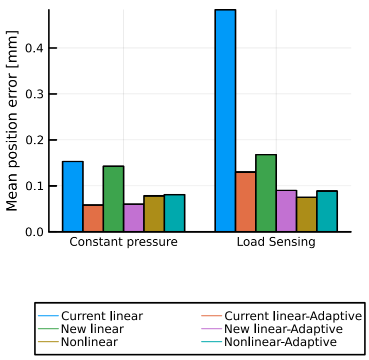

(a) Position

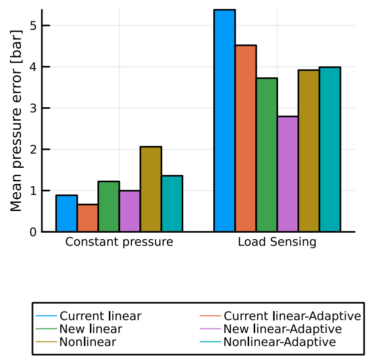

(b) Load pressure

Figure 5.2: Controller performance metrics of the experimental campaign

To validate controller robustness and performance, each control approach was tested under two supply pressure conditions —constant pressure and an active load-sensing system—

mirroring the simulation setup of scenario 2 in Section 4. The experiments were repeated three times per controller and supply pressure scheme, with results averaged to mitigate the influence of outliers.
A comparative evaluation of the controller performances is shown in Figure 5.2. The experimental results generally concur with the simulation outcomes presented in Figure 4.3, thereby, validating the conclusion that both the supply pressure and the adaptive control scheme have a significant influence on performance. A notable discrepancy between the experimental and simulated results is the reduced performance improvement of Type II adaptive position control. This reduction is likely attributable to non-modeled nonlinearities present in the physical system.
In summary, the experimental campaign successfully validated the capabilities of both adaptive and nonlinear controllers to improve accuracy and robustness under real-world conditions.

6. Conclusion

This work presented two novel approaches for the adaptive control of servo-valve controlled hydraulic cylinders. Performance of these designs was analyzed and validated through both numerical simulations and an extensive experimental campaign on a production-grade 4-roll plate bending machine.
The results demonstrate that the proposed adaptive control frameworks significantly enhance accuracy and robustness against a wide range of external disturbances and parametric uncertainties, including external forces, increasing leakages or varying supply pressures. The adaptive gain transfer mechanism, a key contribution of this work, was also validated through simulation, showing improved accuracy and a smooth transition during the crucial switching phase between position and load pressure control.
The experimental campaign, comparing the novel adaptive controllers against conventional linear and nonlinear designs, underscores the practical applicability of the proposed methods. Notably, it was shown that an adaptive enhancement of existing, industrial linear controllers, specifically using the Type II approach, can lead to a significant and verifiable improvement in control accuracy. This finding highlights a clear path for integrating advanced adaptive control into real-world industrial applications without requiring a complete overhaul of existing control systems.

7. References

[1] Gebhardt Norbert; Weber, Jürgen, *Hydraulik – Fluid-Mechatronik: Grundlagen, Komponenten, Systeme, Messtechnik und virtuelles Engineering*, Springer Berlin Heidelberg, 2020.

[2] Jelali, Mohieddine and Kroll, Andreas, *Hydraulic Servo-systems*, Springer London, 2003.

[3] Lohse, Harald, *Modellierung hydraulischer Tiefziehpressen für Prozesskopplung, Reglerauslegung und energetische Bilanzierung*, 1. Aufl., Fluidmechatronische Systeme, Aachen: Shaker, 2015, 186 pp.

[4] Helmke, Marcus et al., *Computer-assisted modeling and automatic controller adjustment for hydraulic drives based on an innovative nonparametric identification method*, Universitätsbibliothek der RWTH Aachen, 2018.

[5] Borrelli, Mauro et al., “MPC load control for aircraft actuator testing”, in: *2020 7th International Conference on Control, Decision and Information Technologies (CoDIT)*, IEEE, June 2020, pp. 587–592.

[6] Gücker, Jan Ulrich, ed., *Experimentelle Identifikation und nichtlineare Regelung eines einachsigen servohydraulischen Antriebs*, Download lizenzpflichtig, Kassel: Kassel Univ. Press, 2006.

[7] Komsta, Jan, Oijen, Nils van, and Antoszkiewicz, Peter, “Integral sliding mode compensator for load pressure control of die-cushion cylinder drive”, in: *Control Engineering Practice* 21.5 (May 2013), pp. 708–718.

[8] Mitov, Alexander et al., “Comparison between Model Predictive (MPC) and Model Reference Adaptive Controllers (MRAC) for Electrohydraulic Steering System Implemented as Real-Time Simulink® Program”, in: *IOP Conference Series: Materials Science and Engineering* 1002.1 (Dec. 2020), p. 012034.

[9] Prabel, Robert and Aschemann, Harald, “Nonlinear adaptive backstepping control of two coupled hydraulic servo cylinders”, in: *2014 American Control Conference*, IEEE, June 2014, pp. 1310–1315.

[10] Radermacher, Tobias, “Modellbasierte Vorsteuerungskonzepte für drehzahlvariable hydraulische Antriebe am Beispiel der Kunststoff-Spitzgießmaschine”, PhD thesis, 2022.

[11] Benosman, Mouhacine, “Model-based vs data-driven adaptive control: An overview”, in: *International Journal of Adaptive Control and Signal Processing* 32.5 (Mar. 2018), pp. 753–776.

[12] Lee, Minhyeong et al., “Precision Motion Control of Robotized Industrial Hydraulic Excavators via Data-Driven Model Inversion”, in: *IEEE Robotics and Automation Letters* 7.2 (Apr. 2022), pp. 1912–1919.

[13] Nan, Fang and Hutter, Marco, “Learning Adaptive Controller for Hydraulic Machinery Automation”, in: *IEEE Robotics and Automation Letters* 9.4 (Apr. 2024), pp. 3972–3979.

[14] Föllinger, Otto, *Nichtlineare Regelungen I*, München: De Gruyter Oldenbourg, 1998.

[15] Bierling, Thomas et al., “Comparative Analysis of MRAC Architectures in a Unified Framework”, in: *AIAA Guidance, Navigation, and Control Conference*, 2010.

[16] Föllinger, Otto, *Regelungstechnik, Einführung in die Methoden und ihre Anwendung*, ed. by Konigorski, Ulrich et al., 13., überarbeitete Auflage, Berlin: VDE Verlag GmbH, 2022, 1452 pp.

[17] Holzapfel, Florian, “Nichtlineare adaptive Regelung eines unbemannten Fluggerätes”, de, PhD thesis, Technische Universität München, 2004, p. 282.

[18] Isidori, Alberto, *Nonlinear Control Systems*, 3. ed., [Nachdr.], vol. [1], Berlin: Springer, 2002, 549 pp.

[19] Khalil, Hassan K., *Nonlinear systems*, 2. ed., Upper Saddle River, NJ [u.a.]: Prentice Hall, 1996, 734 pp.

[20] Bezanson, Jeff et al., “Julia: A Fresh Approach to Numerical Computing”, in: *SIAM Review* 59.1 (Jan. 2017), pp. 65–98.

[21] Rackauckas, Christopher and Nie, Qing, “DifferentialEquations.jl–a performant and feature-rich ecosystem for solving differential equations in Julia”, in: *Journal of Open Research Software* 5.1 (2017).

[22] Ma, Yingbo et al., *ModelingToolkit: A Composable Graph Transformation System For Equation-Based Modeling*, 2021.

Biographies

Marcel Steidle received his bachelor's and master's degrees in Mechanical Engineering from the Technical University of Munich (TUM) in 2017 and 2019, respectively. He is currently an automation engineer at Haeusler AG Duggingen, where he is also pursuing his doctoral degree in cooperation with the the Chair of Fluid Mechatronic Systems at TU Dresden. His research focuses on adaptive control and methods for system and parameter identification in industrial hydraulic systems. Additionally, he explores opportunities to improve the energy efficiency of plate roll bending machines.

Patrick Stadler earned a Bachelor's degree in 2016 and a Master's degree in 2018 in Mechanical Engineering from ETH Zürich, with a focus on robotics and control system design. Since 2019, he has been working at Haeusler AG in Duggingen, applying scientific knowledge to enhance industrial applications.

Jürgen Weber received his Dipl.-Ing. and Dr.-Ing. in Mechanical Engineering from the Technical University of Dresden (TU Dresden) in 1986 and 1991, respectively. His early career was spent in academia, serving as a scientific assistant and senior engineer at TU Dresden's Institute for Machine Tools and Institute for Hydraulics and Pneumatics until 1997.

Following a 13-year period in the industry, where he held various leadership roles in hydraulic systems and advanced development, he returned to academia in 2010. He was appointed an University Professor and Director of the Institute of Fluid Power at TU Dresden. In 2018, he took on an additional leadership role as the Director of the Institute of Mechatronic Engineering. Since 2022, he has been the CEO of Construction Future Lab gGmbH, a startup focused on the digitization of construction machinery, further bridging his academic and industrial expertise.